Orbital and Millennial Antarctic Climate Variability over the Past 800,000 Years

J. Jouzel,[1]* V. Masson-Delmotte,[1] O. Cattani,[1] G. Dreyfus,[1] S. Falourd,[1] G. Hoffmann,[1]
B. Minster,[1] J. Nouet,[1] J. M. Barnola,[2] J. Chappellaz,[2] H. Fischer,[3] J. C. Gallet,[2] S. Johnsen,[4,5]
M. Leuenberger,[6] L. Loulergue,[2] D. Luethi,[6] H. Oerter,[3] F. Parrenin,[2] G. Raisbeck,[7] D. Raynaud,[2]
A. Schilt,[6] J. Schwander,[6] E. Selmo,[8] R. Souchez,[9] R. Spahni,[6] B. Stauffer,[6] J. P. Steffensen,[2]
B. Stenni,[10] T. F. Stocker,[6] J. L. Tison,[9] M. Werner,[11] E. W. Wolff[12]

A high-resolution deuterium profile is now available along the entire European Project for Ice Coring in Antarctica Dome C ice core, extending this climate record back to marine isotope stage 20.2, ~800,000 years ago. Experiments performed with an atmospheric general circulation model including water isotopes support its temperature interpretation. We assessed the general correspondence between Dansgaard-Oeschger events and their smoothed Antarctic counterparts for this Dome C record, which reveals the presence of such features with similar amplitudes during previous glacial periods. We suggest that the interplay between obliquity and precession accounts for the variable intensity of interglacial periods in ice core records.

The European Project for Ice Coring in Antarctica (EPICA) has provided two deep ice cores in East Antarctica, one (EDC) at Dome C (1), on which we focus here, and one (EDML) in the Dronning Maud Land area (2). The Dome C drilling [fig. S1 and supporting online material (SOM) text] was stopped at a depth of 3260 m, about 15 m above the bedrock. A preliminary low-resolution δD record was previously obtained from the surface down to 3139 m with an estimated age at this depth of 740,000 years before the present (740 ky B.P.), corresponding to marine isotope stage (MIS) 18.2 (1). Other data, such as grain radius, dust concentration, dielectric profile, and electrical conductivity, as well as chemical data (3), are available down to this depth, and analyses of the entrapped air have extended the greenhouse gas record—i.e., CO_2, CH_4, and N_2O—back to MIS 16, ~650 ky B.P. (4, 5).

We completed the deuterium measurements, δD_{ice}, at detailed resolution from the surface down to 3259.7 m. This new data set benefits from a more accurate dating and temperature calibration of isotopic changes based on a series of recent simulations performed with an up-to-date isotopic model. In turn, this very detailed Antarctic surface temperature record sheds light on climate analyses in four ways: (i) It allows reliable extension of the climate record back to MIS 20.2 (~800 ky B.P.); (ii) it resolves Antarctic millennial variability over eight successive glacial periods; (iii) it allows quantifiable comparison of the strengths of the successive interglacial and glacial periods; and (iv) the improved time scale allows more accurate investigation of the links between Antarctic temperature and orbital forcing.

This detailed and continuous δD_{ice} profile is shown as a function of time in Fig. 1 and on a depth scale in figs. S2 and S3. For our analysis, we adopted a more precise time scale (SOM text), in which EDC3 has a precision of ±5 ky on absolute ages and of ±20% for the duration of events (6, 7). This scale clearly indicates that the Antarctic counterpart of MIS 15.1 was too long by about a factor 2 in EDC2 (1), as already suggested from the comparison with the deep-sea core record (8), whereas the scale confirms the long duration of MIS 11.3 (1).

The deep-sea benthic oxygen-18 record (8) and the δD_{ice} Dome C record are in excellent overall agreement back to ~800 ky B.P. (MIS 20.2), which suggests that our extended EPICA Dome C record now entirely encompasses glacial stage MIS 18 and interglacial MIS 19. This agreement does not hold true for the earlier part of the record below ~3200 m, and we have strong arguments that the core stratigraphy has been disturbed over its bottom 60 m (SOM text). In contrast, the stratigraphic continuity of the record above ~3200 m is supported by all available data,

including preliminary CO_2 and CH_4 measurements performed along the transition between MIS 20.2 and 19 (SOM text). We are thus confident that the Dome C δD record provides an ~800-ky-old reliable climatic record.

Results derived from a series of experiments performed with the European Centre/Hamburg Model General Circulation Model implemented with water isotopes (9) for different climate stages (SOM text) allowed us to assess the validity of the conventional interpretation of ice core isotope profiles (δD or $\delta^{18}O$) from inland Antarctica, in terms of surface temperature shifts (fig. S4). We inferred that the change in surface temperature (ΔT_s) range, based on 100-year mean values, was ~15°C over the past 800 ky, from –10.3°C for the coldest 100-year interval of MIS 2 to +4.5°C for the warmest of MIS 5.5 (Fig. 2). Despite some differences, the three long East Antarctic isotopic records, Dome C, Vostok (10, 11), and Dome F (12), show a very high level of similarity over their common part and the EDC temperature record is expected to be representative of East Antarctica. All glacial stages before 430 ky B.P. are warmer than MIS 2, by ~1°C for MIS 12, 16 and 18 and by ~2°C for MIS 14 (Fig. 2).

We confirm that the early interglacial periods, now including MIS 19, were characterized by less pronounced warmth than those of the past four climatic cycles (1). Whereas peak temperatures in the warm interglacials of the later part of the record (MIS 5.5, 7.5, 9.3, and 11.3) were 2° to 4.5°C higher than the last millennium, maximum temperatures were ~1° to 1.5°C colder for MIS 13, 15.1, 15.5, and 17, reaching levels typical of interstadials, such as 7.1 and 7.3. MIS 19 shows the warmest temperature for the period before T_v (~ –0.5°C). For MIS 11 to MIS 17, with the exception of MIS 15.1, peak warmth occurred at the end of the warm periods in contrast with the more recent interglacials for which earlier peak warmth was typical (Fig. 2).

Although isotopic records from Antarctica do not exhibit the rapid and large climate variability observed in Greenland records for the so-called Dansgaard-Oeschger (DO) events of the last glacial period (13–15), they clearly exhibit millennial-scale variability with muted and more symmetrical events. Synchronization based on gas indicators unambiguously showed that large DO events have Antarctic counterparts (16, 17), and there were indications that shorter events also have such counterparts both from Vostok and Dome C cores (18–20).

The recent high-resolution EDML isotopic profile over the last glacial period has unambiguously revealed a one-to-one correspondence between all these Antarctic Isotope Maxima (AIM) and DO events (2), which with a few exceptions holds true for the EDC core over the entire last glacial period back to DO 25 (Fig. 2 and fig. S5). At Dome C, the typical amplitude of larger events is ~2°C, much lower than for corresponding DO warmings in Greenland, which are often larger than 8°C and as high as 16°C (21, 22).

[1]Laboratoire des Sciences du Climat et l'Environnement/Institut Pierre Simon Laplace, CEA-CNRS–Université de Versailles Saint-Quentin en Yvelines, CE Saclay, 91191, Gif-sur-Yvette, France. [2]Laboratoire de Glaciologie et Géophysique de l'Environnement, CNRS/Université Joseph Fourier, Boîte Postale 96, 38402, Saint Martin d'Hères, France. [3]Alfred Wegener Institute for Polar and Marine Research, Columbusstrasse, D27568 Bremerhaven, Germany. [4]Department of Geophysics, Juliane Maries Vej 30, University of Copenhagen, DK-2100, Copenhagen, Denmark. [5]Science Institute, University of Reykjavik, Dunhaga 3, Reykjavik 107, Iceland. [6]Physics Institute, University of Bern, Sidlerstrasse 5, CH-3012 Bern, Switzerland. [7]Centre de Spectrométrie Nucléaire et de Spectrométrie de Masse/CNRS, Bat 108, 91405, Orsay, France. [8]Department of Earth Sciences, University of Parma, 43100 Parma, Italy. [9]Département des Sciences de la Terre et de l'Environnement, Université Libre de Bruxelles, Brussels, Belgium. [10]Department of Geological, Environmental and Marine Sciences, University of Trieste, 34127 Trieste, Italy. [11]Max Planck Institute for Biogeochemistry, 100164, D7701 Jena, Germany. [12]British Antarctic Survey, High Cross, Madingley Road, Cambridge, CB3 0ET, UK.

*To whom correspondence should be addressed. E-mail: jean.jouzel@lsce.ipsl.fr

Although some AIM events are more prominent in one of the two EPICA sites (fig. S5), they record millennial variability of comparable magnitude (SOM text), despite the fact that EDML is situated in the Atlantic sector whereas Dome C is facing the Indo-Pacific Ocean. Atmospheric circulation and/or efficient circumpolar oceanic currents can contribute to distribute such climatic signals around Antarctica. This detailed comparison between EDC and EDML records further supports the thermal bipolar seesaw hypothesis (23), which postulates that abrupt shutdowns and initiations of the Atlantic meridional overturning circulation produce slow warmings and coolings in the Southern Ocean and Antarctic region.

Our record exhibits quite similar millennial climate variability during the past three glacial periods, in terms of both magnitude and pacing (fig. S5), suggesting this was also the case in the North Atlantic, as indicated by sediment data (24) and inferred from CH_4 data from Antarctic cores (5, 25). Our lower temporal resolution prevents clear detection of small AIM for earlier glacials, but the amplitude of large AIM, thus presumably of large DO events, does not appear to be substantially influenced by the smaller extent of Northern Hemisphere ice sheets before Termination V. In particular, a very well featured sequence is displayed by the additional cycle provided by the extension of the core from 740 and 800 ky B.P. (Fig. 2 and fig. S5) with three well-marked oscillations that have not yet had counterparts identified in the MIS 18 ocean record (8). Finally, our record shows that during each glacial period, AIM events appear once Antarctic temperatures have dropped by at least 4°C below late Holocene temperature (Fig. 2). We suggest that decreases in Antarctic temperature over glacial inceptions modified the formation of Antarctic bottom waters and that the associated reorganization in deep ocean circulation is the key for the onset of glacial instabilities.

Obliquity changes were previously invoked to explain the change in amplitude between glacial and interglacial periods at the time of the Mid-Brunhes Event (MBE), ~430 ky B.P. (1). This key characteristic of the EDC δD record is now fully supported by our 800-ky detailed temperature record and its improved EDC3 time scale (Fig. 3). Dominated by a periodicity of ~100 ky, the power spectra of ΔT_s (fig. S6) also reveal a strong obliquity component and point to the influence of the precession, at least for 0 to 400 ky. The relative strength of the obliquity and 100-ky components increases when going from past to present, which is consistent with the increasing amplitude of obliquity variations over the past 800 ky due to a 1.2-million-year modulation (26). The 40-ky component is particularly strong, accounting for one-third (4.3°C) of the total range of temperature in the 800-ky record (Fig. 3). Also noticeable are its strong coherency with 65°N summer insolation in the obliquity range (0.97) and its substantial ~5-ky lag with respect to obliquity (fig. S7).

Intermediate-complexity climate models indeed capture a high-latitude signature in annual mean temperature in response to extreme configurations of obliquity, albeit half of that observed here (27). With respect to the strong linear relationship between δD and obliquity, the link may be local insolation changes, which at 75°S vary by ~8% up to 14 W/m^2 (28). Such changes in high-latitude insolation may be amplified by associated changes in heat and moisture transport in the atmosphere (including water vapor and sea-ice feedbacks at high latitudes). They can thus generate changes in the density of ocean surface waters and therefore in ocean thermohaline circulation; such processes involve deep ocean heat storage with constants of millennia. Notably, the obliquity components of temperature records from the tropical Pacific and from Antarctica are in phase (29) within age scale uncertainties. They are thus in phase with the mean annual insolation at high latitude but out of phase with the obliquity component of the mean annual insolation in the tropics. This indicates that mechanisms transferring the high-latitude effect of obliquity

Fig. 1. Comparison of the δD Dome C record on the EDC3 time scale (with all data points in light gray and a smoothed curve in black) with the benthic oxygen-18 record (blue) on its own time scale (8). The 3259.7-m δD record, which includes published results down to 788 m (38), benefits from an improved accuracy (1σ of ± 0.5‰) and a

much more detailed resolution of 55 cm all along the core, whereas the previously published record was based on 3.85-m samples (1). The agreement between the two time series back to ~800 ky B.P. justifies the use of oceanic sediment nomenclature (MIS) for describing the ice core record.
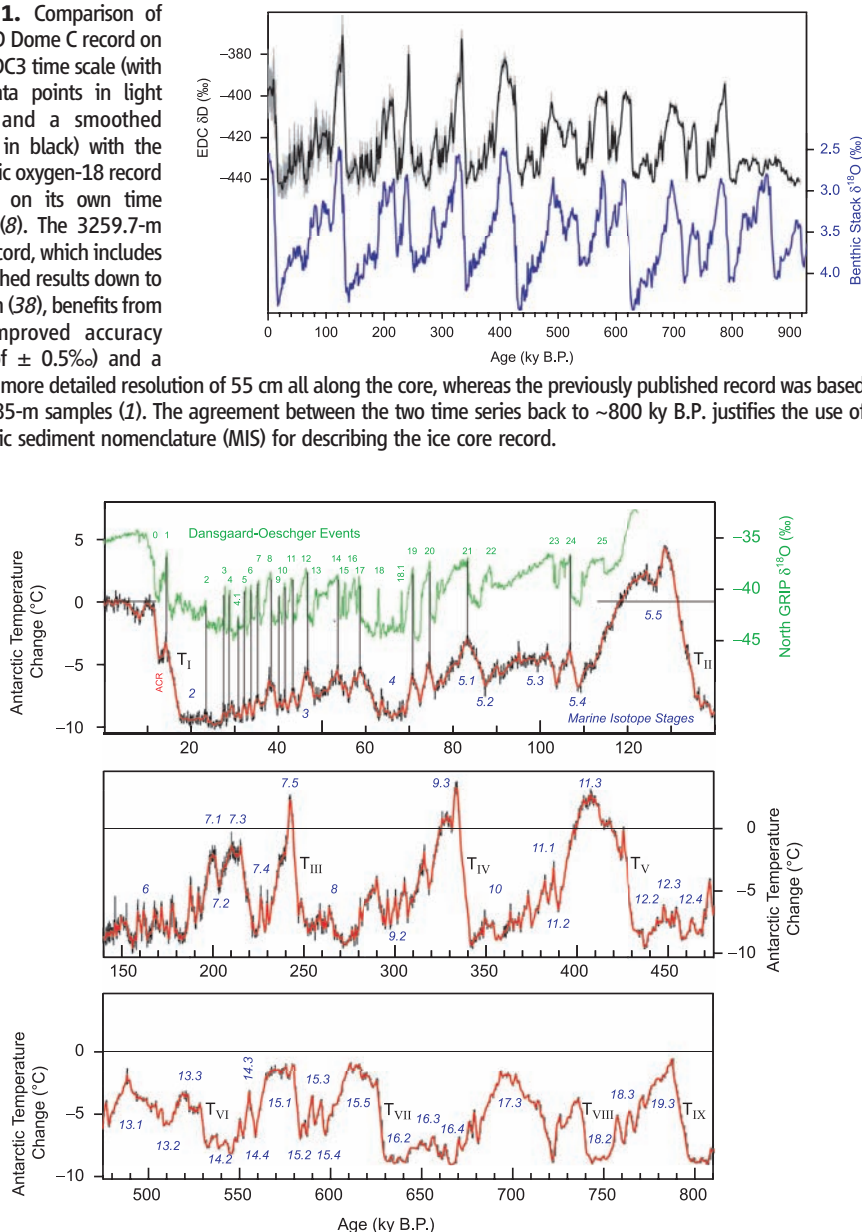

Fig. 2. Dome C temperature anomaly as a function of time over the past 810 ky. Back to 140 ky B.P., we report 100-year mean values, whereas for earlier periods (middle and lower traces), ΔT_s is calculated from 0.55-m raw data; a smooth curve using a 700-year binomial filter is superimposed on this detailed record. In the upper trace (which is plotted on a more highly resolved time axis), we show the correspondence between the DO events as recorded in the North Greenland Ice Core Project isotopic record (2, 15) and AIM events recorded in the EDC temperature record during the last glacial period and the last deglaciation. We have indicated the successive MIS, and the transitions are labeled from T_I to T_{IX}.

toward the tropics may involve changes in heat export from the tropics.

Our EDC ice core shows no indication that greenhouse gases have played a key role in such a coupling. Not only does the obliquity component of the radiative forcing—calculated accounting for both CO_2 and CH_4 changes (30)—have a small amplitude over the past 650 ky (~0.5 W/m², Fig. 3) but it also seems to lag Antarctic and tropical temperature changes. Nor can this in-phase temperature behavior be explained by local insolation, given that this parameter is in anti-phase between low and high latitudes. Rather than assuming that this is caused by greenhouse coupling, we suggest that it results from a transfer of the high-latitude obliquity signal to the tropics through rapid processes involving atmospheric circulation or intermediate oceanic waters, possibly linked, as documented from present-day climates (31) and examined for past climates (32), with changes in sea-ice around Antarctica. The amplitude of the radiative greenhouse forcing, however, is very important in the 100-ky band (~2.5 W/m² comparable to the additional greenhouse forcing due to anthropogenic activities).

This points to a strong carbon-cycle feedback involved in the magnitude and possibly duration of ice ages (33) and to a global character of the Antarctic temperature record.

One key question in this frequency band concerns the relative role of the different orbital parameters in driving terminations. Some authors suggest that terminations occur at multiples of obliquity (34, 35) or precession cycles (36). The latter includes the insolation canon hypothesis that calls upon the interplay of precession and obliquity with considerations of total energy input and threshold effects (37). With our current age scale, the insolation canon approach works well for T_I to T_{IV} but not for earlier terminations. We support the view of combined effects of precession and obliquity in driving ice age dynamics but suggest that the role of obliquity is underestimated by this approach [e.g., high-latitude insolation should not be considered for mid-month but integrated over several months (35)].

The strength of interglacials is highly variable along the record. We suggest that this variation results from an interplay between obliquity and precession (Fig. 3). When 65°N summer insolation (or the inverted precession parameter) and obliquity changes peak in phase (within 5 ky), their combined effects induce strong interglacial periods (MIS 1, 5, 9, 11, and 19). When they are in antiphase, compensating effects induce weak interglacial intensities (MIS 13, 15, 17, and 7.3). In this line, we calculated for each interglacial the cumulative warmth defined with respect to a temperature threshold; we then explored the relationship between this index and insolation. This analysis accounts for the effects of both precession (in the timing of glacial-interglacial transitions) and obliquity (through the mean annual high-latitude insolation). The most robust result is obtained when comparing the cumulative warmth with the cumulative high-latitude insolation (above its average value and taking into account the phase lag of 5 ky). Whereas for small changes in insolation, there is no clear relationship between these two, a linear relationship is observed when the cumulative insolation is larger than ~1700 GJ/m² (fig. S8). In turn, we suggest a causal link between the change of amplitude observed in the EDC temperature record and the modulated amplitude of obliquity.

Our new high-resolution Antarctic climate record is able to resolve systematic long-term as well as millennial changes over the past 800,000 years. Whereas the former may be controlled by local insolation changes largely induced by the obliquity cycle, the latter are induced by changes in North Atlantic deep water formation through the thermal bipolar seesaw. Clearly shown for the last glacial cycle, this is also suggested for earlier glacial periods. Overall, our Antarctic temperature record points to an active role for high southern latitudes in the dynamics of climate change both at orbital and millennial time scales, rather than to a picture of these polar regions simply recording variability originating from other parts of the climate system. This climate record will now serve as a benchmark for exploiting the many properties that are, or will be in the near future, measured on the Dome C core, both in the ice (elemental and isotopic composition of dust and of chemical compounds) and in the gas phase (records of greenhouse gases, other atmospheric compounds, and their isotopic signatures).

Fig. 3. (**A**) Precession parameter displayed on an inversed vertical axis (black line). (**B**) EDC temperature [solid line, rainbow colors from blue (cold temperatures) to red (warm temperatures)] and its obliquity component extracted using a Gaussian filter within the frequency range 0.043 ± 0.015 ky⁻¹ [dashed red line, also displayed in (D) as a solid red line on a different scaling]. Red rectangles indicate periods during which obliquity is increasing and precession parameter is decreasing. (**C**) Combined top-of-atmosphere radiative forcing due to CO_2 and CH_4 (solid blue) and its obliquity component [dashed blue, also displayed in (D) as a solid blue line on a different scaling]. (**D**) Obliquity (solid black line), obliquity component of EDC temperature (red line), and obliquity component of the top-of-atmosphere radiative forcing due to CO_2 and CH_4 (blue). Insolations were calculated using the Analyseries software (39).

References and Notes
1. EPICA Community members, *Nature* **429**, 623 (2004).
2. EPICA Community members, *Nature* **444**, 195 (2006).
3. E. W. Wolff *et al.*, *Nature* **440**, 491 (2006).
4. U. Siegenthaler *et al.*, *Science* **310**, 1313 (2005).
5. R. Spahni *et al.*, *Science* **310**, 1317 (2005).
6. F. Parrenin *et al.*, *Clim. Past* **3**, 243 (2007).
7. G. Dreyfus *et al.*, *Clim. Past* **3**, 341 (2007).
8. L. Lisiecki, M. E. Raymo, *Paleoceanography* **20**, PA1003 (2005).
9. G. Hoffmann, M. Werner, M. Heimann, *J. Geophys. Res.* **103**, 16871 (1998).
10. J. R. Petit *et al.*, *Nature* **399**, 429 (1999).
11. D. Raynaud *et al.*, *Nature* **436**, 39 (2005).
12. O. Watanabe *et al.*, *Nature* **422**, 509 (2003).
13. W. Dansgaard *et al.*, *Nature* **364**, 218 (1993).
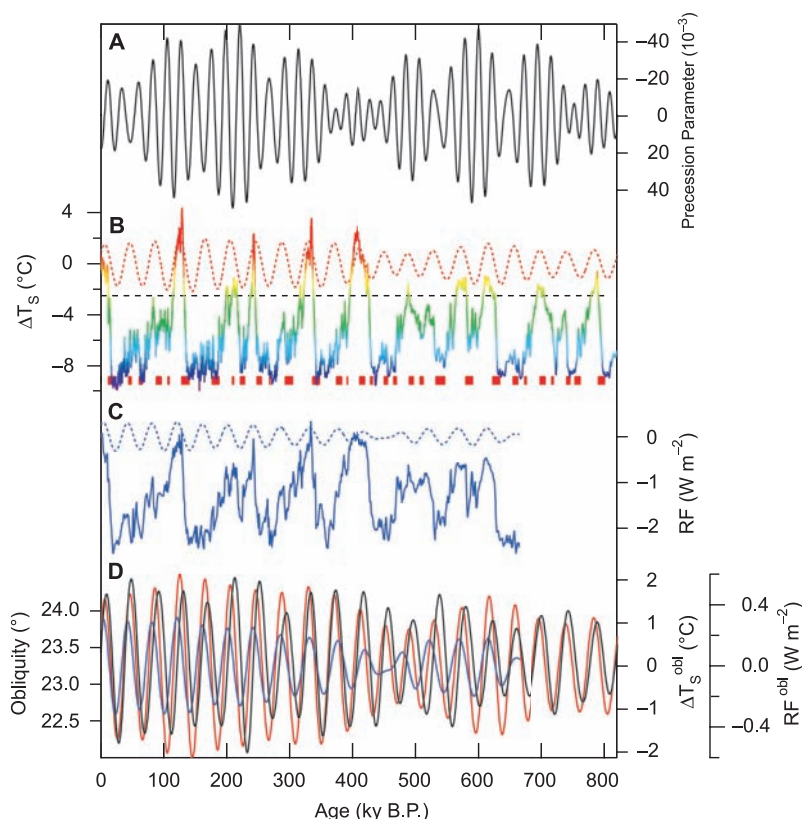14. P. M. Grootes, M. Stuiver, J. W. C. White, S. J. Johnsen, J. Jouzel, *Nature* **366**, 552 (1993).

15. North Greenland Ice-core project (NorthGRIP), *Nature* **431**, 147 (2004).
16. T. Blunier, E. J. Brook, *Science* **291**, 109 (2001).
17. N. Caillon *et al.*, *Geophys. Res. Lett.* **30**, 1899 (2003).
18. F. Yiou *et al.*, *J. Geophys. Res.* **102**, 26783 (1997).
19. M. Bender, B. Malaizé, J. Orchado, T. Sowers, J. Jouzel, in *Geophys. Monogr. Am. Geophys. Union 112*, P. U. Clark, R. S. Webb, L. D. Keigwin, Eds. (American Geophysical Union, Washington, DC, 1999), pp. 149–164.
20. B. Stenni *et al.*, *Earth Planet. Sci. Lett.* **217**, 183 (2004).
21. A. Landais, J. Jouzel, V. Masson-Delmotte, N. Caillon, *CRAS* **377**, 947 (2005).
22. C. Huber *et al.*, *Earth Planet. Sci. Lett.* **243**, 504 (2006).
23. T. Stocker, S. J. Johnsen, *Paleoceanography* **18**, 1087 (2003).
24. M. Delmotte *et al.*, *J. Geophys. Res.* **109**, D12104 (2004).
25. J. F. McManus, D. W. Oppo, J. L. Cullen, *Science* **283**, 971 (1999).
26. H. Palike, N. J. Shackleton, U. Rohl, *Earth Planet. Sci. Lett.* **193**, 589 (2001).
27. V. Masson-Delmotte, *Clim. Past* **2**, 145 (2006).
28. A. L. Berger, *J. Atmos. Sci.* **35**, 2362 (1978).
29. M. Medina-Elizalde, D. Lea, *Science* **310**, 1009 (2005).
30. The radiative forcing is calculated using the mathematical formulation described in F. Joos, *PAGES News*, **13**, 11 (2005).
31. X. J. Yuan, D. G. Martinson, *J. Clim.* **13**, 1697 (2000).
32. S. Y. Lee, C. Poulsen, *Earth Planet. Sci. Lett.* **248**, 253 (2006).
33. F. Parrenin, D. Paillard, *Earth Planet. Sci. Lett.* **214**, 243 (2003).
34. P. Huybers, C. Wunsch, *Nature* **434**, 491 (2005).
35. P. Huybers, *Science* **313**, 508 (2006).
36. M. E. Raymo, L. E. Lisiecki, K. H. Nisancioglu, *Science* **313**, 492 (2006).
37. K. G. Schulz, R. E. Zeebe, *Earth Planet. Sci. Lett.* **249**, 326 (2006).
38. J. Jouzel *et al.*, *Geophys. Res. Lett.* **28**, 3199 (2001).
39. D. Paillard, L. Labeyrie, P. Yiou, *Eos Trans. AGU* **77**, 379 (1996).
40. This work is a contribution to EPICA, a joint European Science Foundation/European Commission (EU) scientific program, funded by the EU and by national contributions from Belgium, Denmark, France, Germany, Italy, The Netherlands, Norway, Sweden, Switzerland, and the UK. This is EPICA publication number 181. This work has in particular benefited from the support of EPICA-MIS of the European 6th framework and Agence Nationale de la Recherche (ANR), Integration des Constraintes Paléoclimatiques pour Réduire les Incertitudes sur l'Evolution du Climat pendant les Périodes Chaudes (PICC). The main logistic support was provided by Institut Polaire Français Paul-Emile Victor and Programma Nazionale Ricerche in Antartide (at Dome C) and Alfred Wegener Institute (at Dronning Maud Land). We thank the Dome C logistics teams (led by late M. Zucchelli and G. Jugie) and the drilling team that made the science possible. This work has benefited from discussions with H. Pälike.

Improved Surface Temperature Prediction for the Coming Decade from a Global Climate Model

Doug M. Smith,* Stephen Cusack, Andrew W. Colman, Chris K. Folland, Glen R. Harris, James M. Murphy

Previous climate model projections of climate change accounted for external forcing from natural and anthropogenic sources but did not attempt to predict internally generated natural variability. We present a new modeling system that predicts both internal variability and externally forced changes and hence forecasts surface temperature with substantially improved skill throughout a decade, both globally and in many regions. Our system predicts that internal variability will partially offset the anthropogenic global warming signal for the next few years. However, climate will continue to warm, with at least half of the years after 2009 predicted to exceed the warmest year currently on record.

It is very likely that the climate will warm over the coming century in response to changes in radiative forcing arising from anthropogenic emissions of greenhouse gases and aerosols (*1*). There is, however, particular interest in the coming decade, which represents a key planning horizon for infrastructure upgrades, insurance, energy policy, and business development. On this time scale, climate could be dominated by internal variability (*2*) arising from unforced natural changes in the climate system such as El Niño, fluctuations in the thermohaline circulation, and anomalies of ocean heat content. This could lead to short-term changes, especially regionally, that are quite different from the mean warming (*3–5*) expected over the next century in response to anthropogenic forcing. Idealized studies (*6–12*) show that some aspects of internal variability could be predictable several years in advance, but actual predictive skill assessed against real observations has not previously been reported beyond a few seasons (*13*).

Met office Hadley Centre, FitzRoy Road, Exeter, Ex1 3PB, UK.

*To whom correspondence should be addressed. E-mail: doug.smith@metoffice.gov.uk

Global climate models have been used to make predictions of climate change on decadal (*14*, *15*) or longer time scales (*4*, *5*, *16*), but these only accounted for projections of external forcing, neglecting initial condition information needed to predict internal variability. We examined the potential skill of decadal predictions using the newly developed Decadal Climate Prediction System (DePreSys), based on the Hadley Centre Coupled Model, version 3 (HadCM3) (*17*), a dynamical global climate model (GCM). DePreSys (*18*) takes into account the observed state of the atmosphere and ocean in order to predict internal variability, together with plausible changes in anthropogenic sources of greenhouse gases and aerosol concentrations (*19*) and projected changes in solar irradiance and volcanic aerosol (*20*).

We assessed the accuracy of DePreSys in a set of 10-year hindcasts (*21*), starting from the first of March, June, September, and December from 1982 to 2001 (*22*) inclusive (80 start dates in total, although those that project into the future cannot be assessed at all lead times). We also assessed the impact of initial condition information by comparing DePreSys against an additional hindcast set (hereafter referred to as NoAssim), which is identical to DePreSys but does not assimilate the observed state of the atmosphere or ocean. Each NoAssim hindcast consists of four ensemble members, with initial conditions at the same 80 start dates as the DePreSys hindcasts taken from four independent transient integrations (*3*) of HadCM3, which covered the period from 1860 to 2001 (*18*). The NoAssim hindcasts sampled a range of initial states of the atmosphere and ocean that were consistent with the internal variability of HadCM3 but were independent of the observed state. In contrast, the DePreSys hindcasts were initialized by assimilating atmosphere and ocean observations into one of the transient integrations (*18*). In order to sample the effects of error growth arising from imperfect knowledge of the observed state, four DePreSys ensemble members were initialized from consecutive days preceding and including each hindcast start date (*23*). Fig. S1 summarizes our experimental procedure.

We measured the skill of the hindcasts in terms of the root mean square error (RMSE) (*24*) of the ensemble average and tested for differences over our hindcast period between DePreSys and NoAssim that were unlikely to be accounted for by uncertainties arising from a finite ensemble size and a finite number of validation points (*18*). We found that global anomalies (*25*) of annual mean surface temperature (T_s) were predicted with significantly more skill by DePreSys than by NoAssim throughout the range of the hindcasts (compare the solid red curve with the blue shading in Fig. 1A). Averaged over all forecast lead times, the RMSE of global annual mean T_s is 0.132°C for NoAssim as compared with 0.105°C for DePreSys, representing a 20% reduction in RMSE and a 36% reduction in error variance (E). Furthermore, the improvement was even greater for multiannual means: For 5-year means, the RMSE was reduced by 38% (a 61% reduction in E), from 0.106°C to

Orbital and Millennial Antarctic Climate Variability over the Past 800,000 Years

J. Jouzel, V. Masson-Delmotte, O. Cattani, G. Dreyfus, S. Falourd, G. Hoffmann, B. Minster, J. Nouet, J. M. Barnola, J. Chappellaz, H. Fischer, J. C. Gallet, S. Johnsen, M. Leuenberger, L. Loulergue, D. Luethi, H. Oerter, F. Parrenin, G. Raisbeck, D. Raynaud, A. Schilt, J. Schwander, E. Selmo, R. Souchez, R. Spahni, B. Stauffer, J. P. Steffensen, B. Stenni, T. F. Stocker, J. L. Tison, M. Werner, and E. W. Wolff

View the article online
https://www.science.org/doi/10.1126/science.1141038
Permissions
https://www.science.org/help/reprints-and-permissions